Combining Benzyl Alcohol Oxidation Saturation Kinetics and Hammett Studies as Mechanistic Tools for Examining Supported Metal Catalysts

Akbar Mahdavi-Shakib[A,B], Janine Sempel[A], Lauren Babb[A], Aisha Oza[A], Maya Hoffman[A], Todd N. Whittaker[B], Bert D. Chandler[B,*], and Rachel Narehood Austin[A,*]

[A]Department of Chemistry, Barnard College of Columbia University, 3009 Broadway, New York, NY 10027, USA

[B]Department of Chemistry, Trinity University, San Antonio, TX 78212-7200

[*]To whom correspondence should be addressed:

raustin@barnard.edu (212) 854-4879 phone

bchandle@trinity.edu (210) 999-7557 phone; (210) 999-7569 fax

Abstract

Understanding and quantifying how the active sites in supported metal catalysts can be modified is critical for rationally designing catalysts. This problem is particularly complex for reactions that occur at the metal support interface (MSI) due to the multiple chemistries associated with the metal and the support. In this study, we used the oxidation of substituted benzyl alcohol over Au/TiO_2 and Au/Al_2O_3 to probe MSI chemistry. Substituents impacted substrate binding, deprotonation, and the rate-limiting transfer of a hydride from benzyl alcohol to Au, as shown by a combination of Michaelis-Menten (M-M) saturation kinetics and kinetic isotope effects. Hammett studies performed with a single substrate versus those done with two substrates together in competition experiments showed significant differences, which were attributable to stronger competitive adsorption on the support by more electron rich alcohols. The M-M analysis showed alcohol substitution impacts substrate binding and deprotonation equilibria, which in turn affect the number of active alkoxides adsorbed at the MSI. Hammett slopes should therefore be measured under saturating conditions using one substrate at a time. The Hammett slopes measured for heterogeneous systems in this manner agree well with the KIE-Hammett slope relationship determined in homogeneous systems, which provide information on the early or late nature of the transition state. Our results show that the combination of Michaelis-Menten and Hammett techniques for benzyl alcohol oxidation provide mechanistic information associated with the MSI chemistry of supported Au catalysts as well as information on active site electronics.

Keywords: benzyl alcohol oxidation, Hammett studies of heterogeneous catalysts, Au/TiO_2, metal-support interface, Michaelis-Menten studies of heterogeneous catalysts

Introduction

Understanding and quantifying changes to the structural and electronic properties of the catalytic active site is vitally important for rational catalyst design; however, few experimental methods provide direct insight into the chemistry at and near the active site during catalysis. This is particularly true when the active site is associated with the metal-support interface (MSI). The number of MSI sites is only a small fraction of the total number of metal sites, which dramatically complicates structural characterization. Further, chemistry at the MSI is governed by multiple, and often competing factors, including the acid/base property of the oxide support and the electronic character of the metal, which may be affected by interactions with the support.[1-19] Disentangling these complex chemistries been particularly helpful in understanding catalysis over supported Au nanoparticles, where the MSI has been shown to play a key role in many reactions.[13-18]

Hammett studies and Michaelis-Menten (M-M) kinetics can be useful tools for understanding how various structural and electronic effects influence catalytic reactions; however, they have only recently begun to be applied to heterogeneous systems.[20-25] Hammett studies can elucidate subtle mechanistic details in both homogeneous[26-32] and heterogeneous reactions,[33-36] but are just materializing as tools to probe active site electronics[37]. The M-M treatment emerged as an effective tool in enzyme catalysis at a time when little was known about the structure of enzymatic active sites. In this respect, reactions at the MSI are similar to enzymatic reactions because of the structural complexity and multiple types of chemistries potentially involved at the active site. In many cases, the mechanistic and structural details of the active site(s) are unknown. Here we show how principles commonly employed in studying enzyme and homogeneous catalysts can be used to gain insight into the chemistry taking place at MSI during benzyl alcohol oxidation over

supported Au catalysts. For single substrates the M-M equation and the Langmuir-Hinshelwood (LH) equation, which is more commonly used in heterogeneous catalysis, yielded identical results.

The catalyzed oxidation of benzyl alcohol is a well-studied reaction in both homogeneous and heterogeneous systems. In the homogeneous catalysis literature, several groups have reported KIE values for the benzylic H between 1.3 and 5,[27-31, 38] indicating C-H bond breaking is rate determining. Using Pd(IiPr)$(OAc)_2(H_2O)$ (IiPr= 1,3-bis(2,6-diisopropylphenyl)imidazol-2-ylidene) as a catalyst, Mueller *et al*. showed base is required for Pd-catalyzed alcohol oxidations in their system,[27] and went on to provide strong mechanistic evidence for alcohol deprotonation followed by hydride transfer.[27] Using a $Pd(OAc)_2$/Pyridine catalyst system, Stahl's group showed benzyl alcohol can bind to Pd directly, but undergoes rapid deprotonation.[39] In both cases, rate-limiting hydride transfer occurred from an alkoxide rather than directly from the alcohol. Sigman's group also found strong correlations between KIE values and Hammett slopes when hydride transfer is rate limiting.[27, 40] A large Hammett slope (>1) was measured along with a small KIE was interpreted as a late transition state[40], while a large KIE (around 5) and a smaller Hammett slope (around 0.5) was interpreted as an early transition state.[27]

The general mechanistic conclusions from these studies are mirrored in heterogeneous systems, particularly for supported Au catalysts. Several groups have reported primary kinetic isotope effects associated with benzylic hydrogen transfer.[36, 41] Similarly, Abad *et al*. found a linear free energy relationship with $\rho < 0$ over Au/CeO_2[41], as did Fristrup *et al*. over Au/TiO_2.[36] Kumar *et al.* also measured Hammett relationships for Au/ZnO_2, Au/TiO_2, Au/SiO_2, and Au/Al_2O_3.[37] Together with spin trapping experiments by Chechik *et al.*[42], these studies all support the conclusion that hydride transfer from the benzylic carbon is the rate determining step in benzyl alcohol oxidation over supported Au catalysts. DFT calculations also suggest that alcohol

deprotonation is required[37, 43-44], in agreement with the homogeneous catalysis literature.[27, 39, 45] The catalytic cycle is completed through the adsorption of O_2, which reacts with adsorbed hydride to ultimately produce water.[46] Because these steps occur after rate determining hydride transfer, they have smaller impacts on the intrinsic reaction kinetics.

This mechanistic understanding provides a rationale for using a combination of saturation kinetics and Hammett studies to evaluate electronic effects on a catalytic active site. Electronic metal-support interactions (EMSI) can modify active sites on metals.[47-48] Kumar *et al.* showed that experimental Hammett slopes determined on supported Au catalysts scale with the work function of the support.[37] DFT calculations in that study also showed that the transition state in hydride transfer is sensitive to the charge on the accepting Au nanoparticle.[37]

In this work, we use a M-M analysis of benzyl alcohol oxidation to extract K_M and ν_{max} values for substituted benzyl alcohols over Au/TiO_2 and Au/Al_2O_3 catalysts. We show that a combination of M-M kinetics, kinetic isotope effect (KIE) experiments, a Langmuir adsorption analysis, and Hammett studies can be used to evaluate the relative impacts of substrate adsorption, deprotonation, and hydride transfer on the reaction rate. We also compare results from substrate competition experiments, which are often used in Hammett studies[26, 36, 49-50], to more traditional single substrate experiments. Comparing these two methods reveals important considerations regarding substrate binding to the catalysts[49-50] and provides insight into the interplay between substrate adsorption and deprotonation that differentiates heterogeneous from homogeneous systems. This analysis facilitated the extraction of reliable hydride transfer rate constants, which places the heterogeneous Hammett slope-KIE relationship squarely in line with that of homogeneous systems.

Results and Discussion:

Two catalysts, commercially available 1% Au/TiO_2 and freshly prepared 1% Au/Al_2O_3 were studied in this work. Characterization details for the Au/TiO_2 catalyst, which has average Au nanoparticle size of 2.7 ± 1 nm, have been previously reported.[37] The Au/Al_2O_3 was prepared via deposition-precipitation as described previously.[51-52] Transmission electron microscopy (TEM) indicated similar but slightly smaller Au particle sizes (1.8 ± 0.4 nm) for the Au/Al_2O_3 catalyst. Preparation details and representative TEM images are available in the supporting information.

Alcohol oxidation kinetics were studied at 60 °C in batch reactors using toluene as solvent; see supporting information for details. Measured rates were insensitive to the stirring rate and scaled with the catalyst mass, indicating the reaction is not limited by external mass transfer or mass transfer between the liquid and gas phases. The reaction is 0^{th} order with respect to O_2 under our conditions. This, along with the saturation kinetics observed for benzyl alcohol similarly indicate the reaction is not limited by internal mass transport. Typical experimental uncertainty in measured rates is ~ 20%; see supporting information for further details.

Michaelis-Menten analysis of single substrate experiments. Figure 1 shows the reaction rate dependence on substrate concentration (saturation plots) for 4-methoxylbenzyl alcohol (CH_3O-BA), 4-methoxylbenzyl-α,α-D_2 alcohol (CH_3O-α,α-D_2 BA), and 4-(trifluoromethyl) benzyl alcohol (CF_3-BA) over the Au/TiO_2 catalyst. For all substrates, the initial reaction rate (mM/min) increased with the substrate concentration until it reached a maximum value, indicating the reaction becomes kinetically saturated, Figure 1.

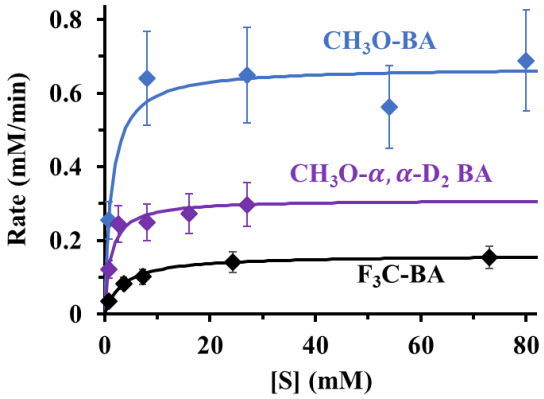

Figure 1. Saturation plots of Au/TiO_2. The symbols are experimental data measured in single substrate reactions; lines are plotted using the extracted K_M and ν_{max} values reported in Table 1.

The saturation kinetics observed in Figure 1 can be described with a generic mechanism similar to the M-M mechanism, as shown in Scheme 1. Applying Scheme 1 to Au catalyzed benzyl alcohol oxidation, C (the catalyst) represents the active site at the MSI of the Au nanoparticle, S represents the substrate, CS' describes the activated alcohol / alkoxide bound at the MSI, and P is the benzaldehyde product. This results in a formal hydride adsorbed to the Au nanoparticle, which subsequently reacts with O_2. Oxygen is constantly supplied to the reaction, and the reaction rate is independent of O_2 pressure under our conditions[37, 53], indicating that Au-H oxidation to re-generate the catalyst is fast and occurs after the rate-determining step.[36-37, 41] Our focus on the mechanistic details of associated with hydride transfer step allows us to examine low conversions; consequently, our simplified scheme does not require inclusion of Au-H oxidation steps to accurately model the kinetic data. The goal of this work is to simplify the reaction network so that we can more readily evaluate the steps leading up to hydride transfer, and ultimately use this information to evaluate differences between catalysts. However, we note that oxygen adsorption and hydride oxidation are important for reactions carried out at higher conversions or with other catalyst systems and should be accounted for under when evaluating the full reaction network.[46]

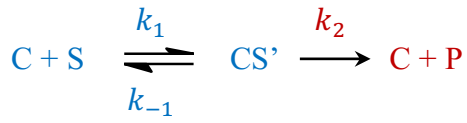

Scheme 1. Michaelis-Menten mechanism

The first step in Scheme 1 is an "assembly equilibrium", which incorporates all substrate adsorption steps and any activation steps required to produce the adsorbed intermediate(s) involved in the rate determining step. In the specific case of benzyl alcohol oxidation, the assembly equilibrium includes alcohol adsorption onto the support and activation of the –OH group, followed by rate determining hydride transfer to that Au nanoparticle.[37] Alcohol activation may involve hydrogen bonding of the alcohol with a basic surface hydroxyl group at or near the metal-support interface, or full deprotonation to an adsorbed alkoxide.[27, 37-38, 43-45, 54] Indeed, several studies have concluded that alcohol deprotonation is required for fast hydride transfer from the benzylic carbon.[27, 37-38, 43-45, 54] Scheme 1 is completely analogous to the M-M treatment of enzymatic catalysis data. As a result, K_M and ν_{max} values can be extracted from double reciprocal (Lineweaver-Burk) plots, see supporting information. The extracted values are summarized in Table 1.

Table 1. K_M and v_{max} values extracted from L-B plots

Catalyst	Substrate	K_M (mM)	ν_{max} (mM min^{-1})	K_{asmb} (M^{-1})
Au/TiO_2	CH_3O-BA	1.3 (±0.1)	0.67 (±0.04)	770 (±60)
	CH_3O-α,α-D_2 BA	1.2 (±0.2)	0.31 (±0.02)	830 (±140)
	F_3C-BA	3.4 (±0.2)	0.16 (±0.01)	290 (±20)
Au/Al_2O_3	CH_3O-BA	3.3 (±0.5)	1.3 (±0.09)	300 (±50)
	F_3C-BA	10 (±2)	0.21 (±0.03)	100 (±20)

We first address the kinetic isotope effect (KIE) data for CH_3O-BA in the context of the M-M parameters. Deuteration of the α hydrogens had no effect on the K_M values, indicating the

"assembly equilibria" leading up to the rate determining step are unaffected by this substitution. Substrate deuteration is unlikely to change the number of active sites on the catalyst, so the ratio of v_{max} values should be a measure of the k_2 rate constants and therefore a measure of the KIE. The measured value of 2.2 ± 0.2 indicates a primary kinetic isotope effect. This value is consistent with previously reported values for heterogeneously catalyzed reactions, which are generally on the order of 1.5 to 2.[36, 41] Conte *et al*. found a larger KIE of 5 in studying 2-propanol oxidation over Au/CeO_2[42]; this value is consistent with some homogeneously catalyzed alcohol oxidations as discussed below.

The M-M analysis provides experimental insight into substitution effects on the binding and deprotonation pre-equilibria; previous studies have not examined these effects. The KIE indicates a factor of two difference in k_H vs k_D; however, there is no change in K_M. Since $K_M = \frac{k_{-1}+k_2}{k_1}$, this indicates $k_{-1} >> k_2$; hence, $K_M \cong \frac{k_{-1}}{k_1} = \frac{1}{K_{asmb}}$, where K_{asmb} is the overall assembly equilibrium. Thus, the isotopic substitution experiment also shows that K_M values can be used to directly evaluate changes to the binding and deprotonation equilibria (K_{asmb}, see below).

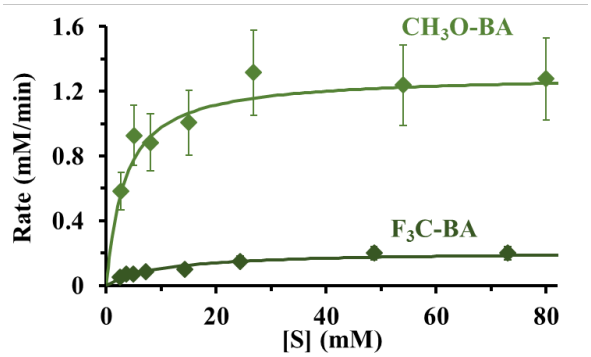

Figure 2. Saturation plots for CH_3O-BA and F_3C-BA oxidation over Au/Al_2O_3 in single substrate experiments. The symbols are the measured rates and lines are M-M plots constructed using the extracted K_M and ν_{max} values reported in Table 1.

Figure 2 shows the saturation plots for CH_3O-BA and F_3C-BA oxidation over Au/Al_2O_3; the extracted K_M and ν_{max} values can be found in Table 1. In spite of the large differences in the substituent electron donating/withdrawing ability, the K_{asmb} values for CH_3O-BA are only about 2-3 times larger than for F_3C-BA. Similarly, the values for the same substrate differ by only about a factor of three on Au/TiO_2 vs. Au/Al_2O_3. Thus, the overall assembly equilibrium is relatively similar regardless of the substituents or the support. This is likely due to a compensation effect between adsorption strength, which is favored by electron rich alcohols, and acidity, which is favored by electron poor alcohols. It is also worth noting the small changes in K_{asmb} correlate with the electron richness of the alcohol, suggesting alcohol adsorption dominates the assembly equilibrium. The adsorption constants determined from K_M values only reflect adsorption at the MSI that leads to reaction, so these values may be influenced by any bonding interactions between the substrate and the catalyst. In this case particular case, that includes any bonding interactions between the pi system and the nanoparticle surface. Arene adsorption is relatively weak on Au surfaces,[55{Yildirim, 2013 #105, 56] but adsorption strength increases as surface atoms become under-coordinated on smaller particles.[57-58] While we believe the adsorption interaction is dominated by hydrogen bonding interactions between the alcohol and the support, we cannot directly ascertain the degree to which arene association to the nanoparticle might affect this adsorption constant.

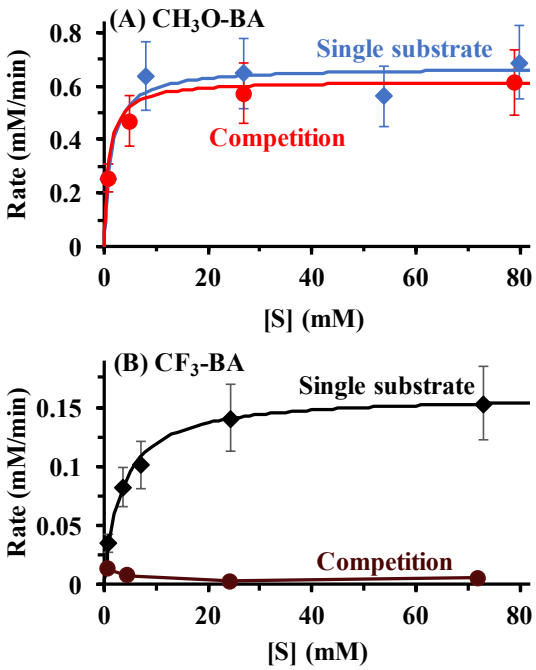

Figure 3. Saturation plots for (A) OCH_3-BA and (B) F_3C-BA during single substrate and competition experiments over Au/TiO_2. Solid lines show fits from extracted M-M parameters; for F_3C-BA in the competition experiment, the solid line is included to guide the eye.

Kinetic analysis of competition experiments. For experimental expediency, Hammett relationships are often measured using competition experiments, in which two (or more) substrates are present in the reaction mixture.[26, 36, 49-50] The competitive adsorption of alcohols can impact several aspects of heterogeneous catalysis, as Friend's group has shown that competitive adsorption of alcohols on Au controls the product distribution in coupling reactions.[59-62] Mao et al. also used competition experiments to examine non-fluorescent reactions over individual nanoparticles.[22] It is therefore important to understand the ways in which completion experiments differ from single substrate experiments, since competition experiments can alter surface reaction pathways. Since there are several literature reports using competition experiments to determine

Hammett parameters in the literature,[26, 36, 49-50] we wanted to evaluate the potential utility of this technique for this particular reaction.

With this goal in mind, we performed experiments using equimolar concentrations of F_3C-BA and CH_3O-BA over Au/TiO_2 to evaluate potential differences between single substrate and competition experiments. Figure 3A shows the saturation plots for CH_3O-BA collected in single substrate and competition experiments are essentially indistinguishable. Extracted K_M and ν_{max} values (Table 2) are the same within experimental errors.

Table 2. Extracted Michaelis-Menten parameters for CH_3O-BA in single substrate and competition (with F_3C-BA) experiments.

	K_M (mM)	ν_{max} (mM min^{-1})
single substrate	1.3 (±0.1)	0.67 (±0.04)
competition	0.9 (±0.6)	0.62 (±0.02)

Figure 3B shows F_3C-BA oxidation is considerably slower in the competition experiments. The measured rates were essentially independent of substrate concentration, making extraction of M-M parameters impossible. These data suggest the mechanism of F_3C-BA oxidation is fundamentally different in the competition experiments. The measured rates are comparable to background substrate oxidation in the absence of an Au catalyst, (see supporting information) indicating the observed reactivity is likely due to uncatalyzed oxidation of F_3C-BA by O_2 in solution.

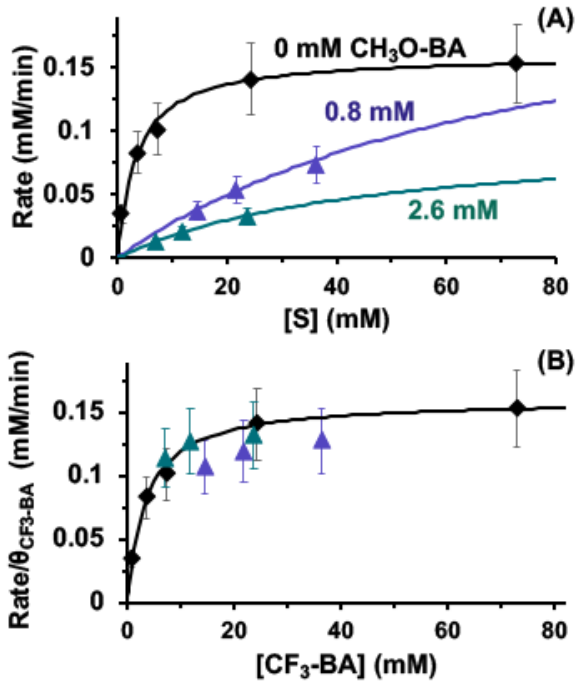

Figure 4. Oxidation of F_3C-BA over Au/TiO_2 in the presence of CH_3O-BA. (A) F_3C-BA saturation plots in the presence of 0, 0.8, and 2.6 mM CH_3O-BA. (B) F_3C-BA oxidation rate normalized to the estimated surface coverage of CF_3-BA.

These data suggest that CH_3O-BA inhibits F_3C-BA oxidation, so we examined F_3C-BA oxidation in the presence of lower concentrations of CH_3O-BA. Saturation plots are shown in Figure 4; extracted K_M and ν_{max} values are presented in Table 3. The consistency in the ν_{max} values indicates that the inhibition does not affect the rate determining step or the number of active sites on the catalyst. Rather, the changes in K_M and K_{asmb} indicate that the competition perturbs the pre-equilibrium processes.

Table 3. Extracted Michaelis-Menten data for F_3C-BA oxidation over Au/TiO_2 in the presence of CH_3O-BA

[CH_3O-BA] (mM)	K_M (mM)	ν_{max} (mM min^{-1})	K_{asmb} (M^{-1})
0	3.0 (± 0.8)	0.16 (±0.01)	330 (± 80)
0.8	46 (± 11)	0.22 (±0.05)	22 (± 5)
2.6	67 (± 16)	0.10 (±0.01)	15 (± 4)

The changes in K_M can be understood with a closer examination of the assembly equilibria. Alcohol substitution induces two competing effects on the two components of the assembly equilibrium. Electron rich alcohols will have higher affinities for metal ions and protons on the support surface. At the same time, more electron rich alcohols are less acidic, which reduces the coverage of the surface alkoxide necessary for hydride transfer to Au. The substituent effects in the single substituent experiments in Table 1 show the K_{asmb} values correlate with the electron richness of the alcohol and that the assembly equilibria are therefore dominated by alcohol binding to the support. The preferential binding of the more electron rich alcohol impacts the competition experiments because surface alcohol coverages in the competition experiments are not necessarily equivalent to the relative solution concentrations. This results in considerably lower and ultimately unfavorable assembly equilibrium constants for F_3C-BA in the presence of CH_3O-BA.

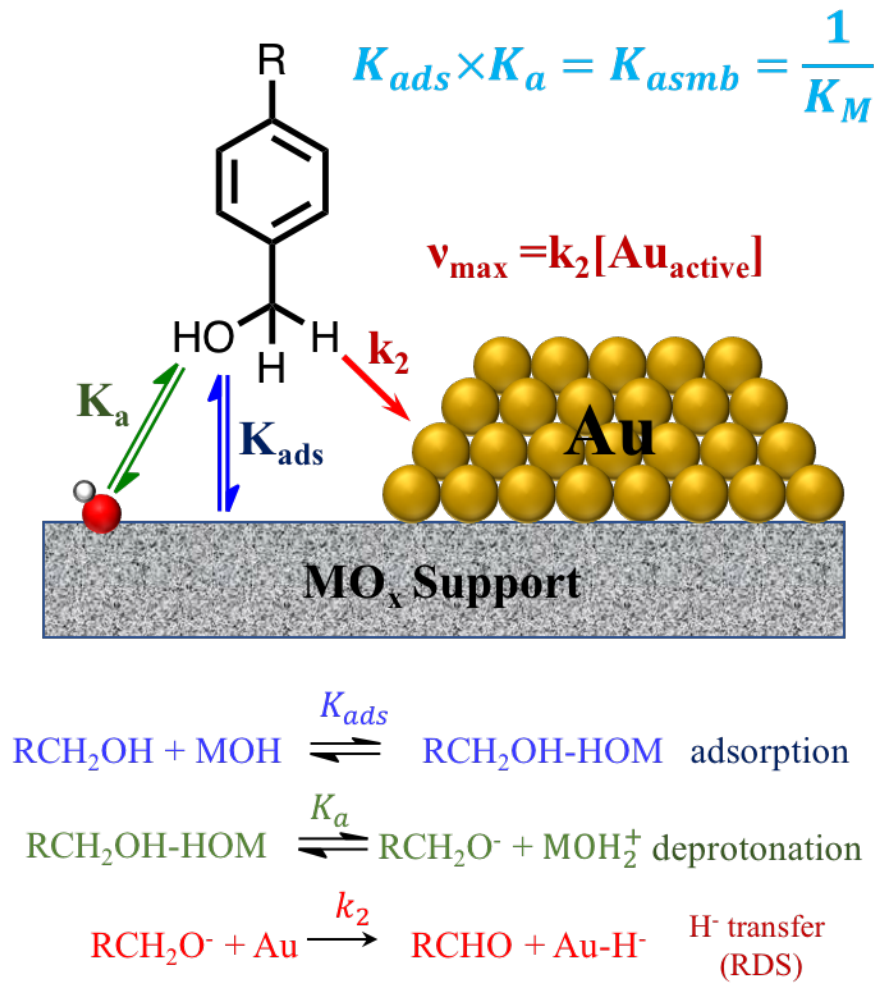

Scheme 2. Relationships between Michaelis-Menten constants and alcohol binding / deprotonation equilibria

To quantitatively evaluate this effect, we decomposed the assembly equilibrium into adsorption and deprotonation equilibria as shown in Scheme 2. Using the determined K_{asmb} values and gas-phase acidity constants, effective adsorption constants (K_{ads}) for alcohol adsorption from toluene to the active site were determined. As Table 4 shows, both adsorption constants are sufficiently large such that, in single substrate experiments, the surface coverage is essentially unity. However, the CH_3O-BA adsorption constant is about 35 times greater than the CF_3-BA

adsorption constant, making competition for active sites important in the mixed substrate experiments.

Table 4. Thermodynamic parameters for alcohol adsorption and deprotonation

	CH_3O-BA	CF_3-BA
K_{asmb}	770 (±60)	330 (± 80)
pK_a[a]	16.59	15.52
K_{ads}	3.0×10^{19}	1.1×10^{18}
θ[b]	0.97	0.03

[a]pK_a values estimated from σ constants as described in reference[63]
[b]surface coverage in equimolar competition experiments

Using a competitive Langmuir adsorption model, the surface coverages of the two alcohols on the support are 0.97 and 0.027, respectively. The rate data from the equimolar competition experiments are consistent with this as they show essentially no F_3C-BA activity and CH_3O-BA activity only slightly slower than in single substrate experiments. We also reevaluated the rate data in Figure 4A by normalizing each data point with the expected coverage based on the competitive Langmuir adsorption model. As Figure 4B shows, all three experiments show comparable coverage-normalized rates.

This analysis allows us to evaluate the relative merits of competition and single substrate experiments. Since ν_{max} values are not affected by the substrate competition, it is possible to extract Hammett relationships from competition experiments over heterogeneous catalysts. However, doing so may introduce errors into both the measurements and their interpretation. Care must be taken to ensure any differences in surface substrate coverage are accounted for; this may require determining the relative surface coverages during the competition experiments. In many cases, higher data quality will be obtained more readily from single substrate experiments.

Table 5. Literature Hammett parameter and KIE values for homogeneous benzyl alcohol oxidation

Catalyst	ρ	KIE	Reference
Pd(IiPr)(OAc)2(H2O)	-0.48	5.5[a]	[27]
Ru(II)/TEMPO	-0.58	5.1	[28]
Ru(II) (Shvo's catalyst)[b]	-0.89	3.7[a]	[29]
Manganese (III) salen	-1.2	2	[30]
Pd (II)/(-)-sparteine	-1.41	1.31[a]	[40]

[a]*sec*-phenethyl alcohol substrate was used for KIE studies. [b]1-Hydroxytetraphenylcyclopentadienyl-(tetraphenyl-2,4-cyclopentadien-1-one)-μ-hydrotetracarbonyldiruthenium(II)

Hammett Slope. We next sought to place the ν_{max} data into the context of the available homogeneous and heterogeneous catalysis literature. Using the ratio of the ν_{max} values to estimate the Hammett slope yields a qualitative ρ value of 0.45 for Au/TiO_2; this value is consistent with previous reports by Kumar *et. al.* (0.44)[37] on the same catalyst and by Corma's group (~0.163) for Au/CeO_2[41].

However, as Table 5 shows, ρ values range widely for homogeneous catalysts and correlate strongly with KIE values. The homogeneous catalysis data in Figure 5 cover five catalyst systems utilizing three different metals (Pd, Ru, and Mn). As such, they suggest that this correlation is diagnostic of the reaction, at least for homogeneously catalyzed systems. While internally consistent with the report from Corma's group, the Hammett slopes obtained using the ν_{max} values, along with Corma's values, do not fit this trend. This raises the question: is this due an intrinsic difference in the reaction over supported Au catalysts, or are there additional factors should be considered when determining Hammett slopes over heterogeneous catalysts?

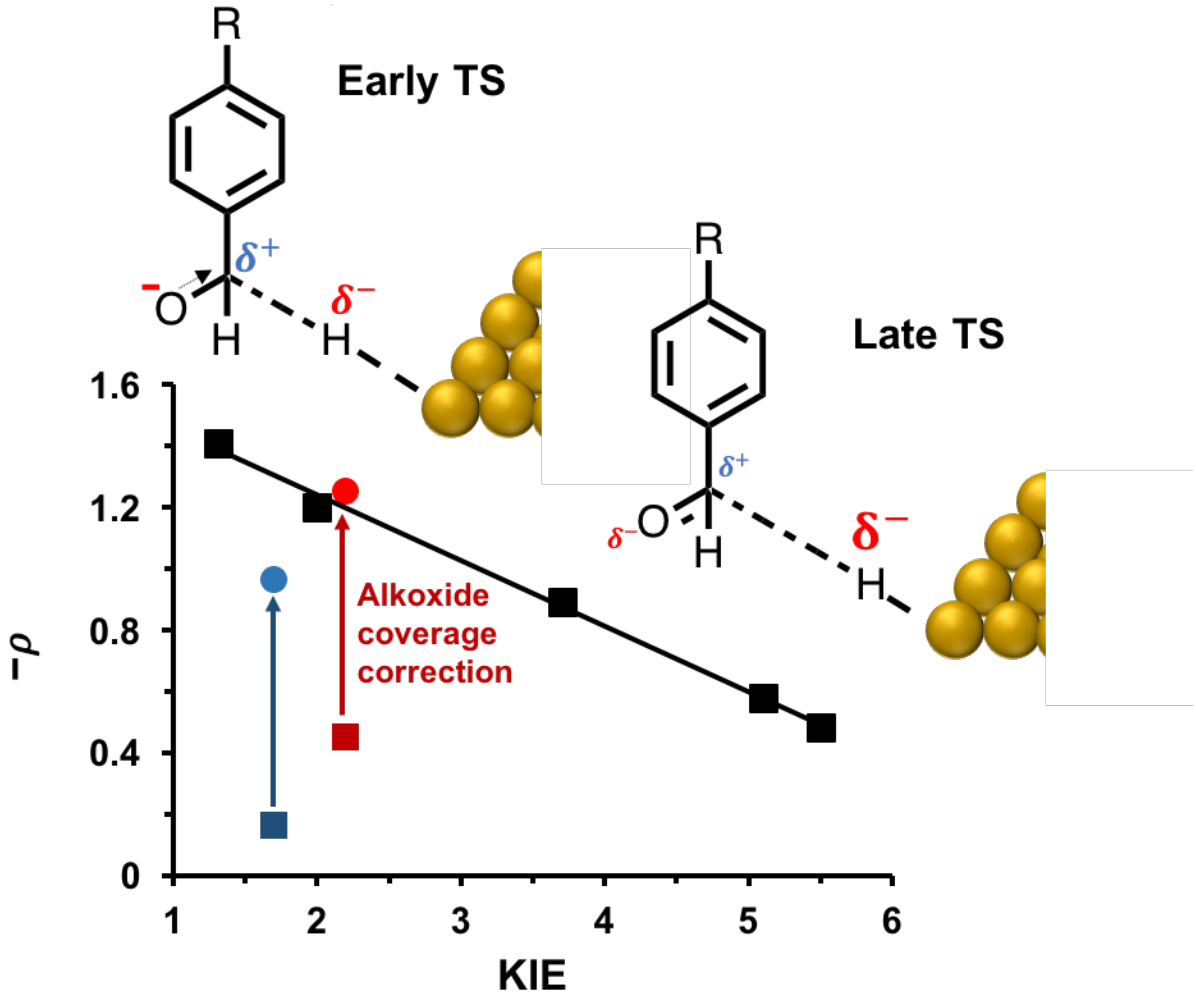

Figure 5. Correlation between Hammett slope and KIE. The black symbols are for homogeneous benzyl alcohol oxidation literature summarized in Table 5. The blue square is for the heterogeneous benzyl alcohol oxidation reported by Abad *et al*.[41] and the red square is for the ν_{max} value measured in this work. The blue and red circles are the same data after normalizing the data to the expected differences in surface alkoxide coverage based on substrate pK_a values.

The current study allows us to carefully consider the assumptions associated with applying Hammett studies to heterogeneous catalysts. In particular, using the ν_{max} values in a Hammett analysis involves an inherent assumption that the number of active sites does not change when the substrate changes. This is a reasonable assumption from the standpoint of the structural requirements of the catalytic active site at the MSI – there is no reason to think that these structural requirements of the catalytic active site would change from one substrate to the next provided there are no significant steric differences in the substrates.[37]

This assumption is imperfect for evaluating the rate constant for hydride transfer to Au (k_2), which is the ultimate goal of this Hammett study, because ν_{max} is formally defined as $k_2*[Au_{active}]$. Since the reaction mechanism invokes hydride transfer from a surface alkoxide to the Au nanoparticle, the amount of active Au depends on surface alkoxide concentration, and therefore on the substrate pK_a. Consequently, accurate extraction of k_2 values requires accounting for differences in alkoxide surface coverage that arise from the pK_a values for individual substrates. In the specific example here, both alcohols (F_3C-BA and CH_3O-BA) have adsorption equilibrium constants sufficiently large that the alcohol surface coverage will always be close to unity in typical single substrate experiments. However, the greater acidity of F_3C-BA will lead to a greater number of active F_3C-substituted alkoxides (relative to CH_3O-BA alkoxides), regardless of the support used. The ν_{max} value for F_3C-BA will therefore overestimate k_2 relative to CH_3O-BA, resulting in an underestimation of the true Hammett slope.

Determining the true surface coverage of alkoxide at the MSI will be challenging. However, since Hammett relationships fundamentally examine changes in rate constants, determining the true alkoxide surface coverage is not necessary if the relative changes can be estimated. We used a simple numerical model to examine the relative influence of pK_a, pK_b (of a

H^+ accepting support), K_w, and concentration on the ratio of the conjugate base concentration of two acids (supporting information). While the absolute alkoxide concentrations change considerably with conditions, and this simplified model does not account for surface charging, it highlights two key results. First, the pK_b of the base has no effect on the alkoxide ratio. Provided surface charging effects are not substantially different, which is reasonable given that both the proton and conjugate base reside on the support surface, the relative ratios of alkoxides will be the same on a given support. Second, it therefore follows that the ratio of conjugate bases (the alkoxides) depends only on the difference between the two pK_a values of the two acids. While these effects are significant, they are readily quantifiable. Using Cohen's method to estimate the pKa values for the two alcohols[63], using the gas-phase acidity constants, the ratio of [F_3C-BA]/[CH_3O-BA] is calculated to be ~10. Since the identity of the base does not affect this value, it reflects a reasonable estimate of the differences in surface alkoxide coverage on any given support.

Table 6. K_M and ν_{max} values extracted from M-M plots

Catalyst	Substrate	ν_{max} (mM min^{-1})	k_{2rel} (mM min^{-1})	$-\frac{\Delta\log(\nu_{max})}{\Delta\sigma^+}$	$-\rho$
Au/TiO_2	CH_3O-BA	0.67 (±0.04)	8.6 (±0.5)	0.45 (±0.03)	1.25 (±0.03)
	F_3C-BA	0.16 (±0.01)	0.16 (±0.01)		
Au/Al_2O_3	CH_3O-BA	1.3 (±0.1)	17 (± 1)	0.57 (±0.05)	1.37 ± (0.05)
	F_3C-BA	0.21 (±0.03)	0.21 (±0.03)		

Table 6 shows the determined Hammett slope (ρ) using both the ν_{max} values and the relative k_2 values (k_{2rel}), which normalize the CH_3O-BA ν_{max} value to the pK_a difference. As Figure 5 shows, the extracted ρ values using k_{2rel} for our catalyst and applying the same correction to Corma's study are largely in line with correlation to KIE observed in homogeneous studies. We also note the correction increases the magnitude of the Hammett parameter, but not the measured

difference between the supports. Thus, the interpretation of the differences between ρ values associated with various supports does not change: relative to Au/TiO_2, Au/Al_2O_3 is better able to stabilize the developing hydride, resulting in a more negative ρ value and a faster reaction rate.

Finally, the correlation between ρ and the KIE provides insight into the reaction that may help improve future catalyst design. Drawing on the Hammond Postulate,[64] the two techniques are closely correlated because both assess the position of the transition state for a particular catalyst system, but by examining different chemical properties of that transition state. The KIE reports on the degree of C-H bond breaking in (or the "flatness" of) the transition state, while ρ reports on the degree of charge buildup on the benzylic carbon in the transition state. In this case, early transition states are characterized by relatively small KIE values because the vibrational energy associated with the C-H bond largely resembles the reactant alcohol. The early stage of the hydride transfer results in development of a partial positive charge on the benzylic carbon, which is sensitive to the electron donating or withdrawing ability of the aryl substituent.

In contrast, late transition states are associated with nearly complete hydride transfer to the metal and concomitant C-H bond scission. Since the C-H(D) bond is largely broken, the transition state has very little C-H(D) bond character, and therefore minimal differences in the isotopic zero-point energies, resulting in a large KIE. Late transition states have significant carbonyl bond formation, which reduces the net charge on the benzylic carbon. The smaller Hammett slope indicates the relative insensitivity to the aryl substituents. This suggests supports capable of both improving the ability of Au to stabilize the hydride transfer and increasing either the concentration of the active alkoxide at the MSI or increasing alkoxide reactivity may prove to be superior alcohol oxidation catalysts.

Conclusion

This work uses Michaelis-Menten kinetics to evaluate electronic changes to alcohol adsorption, deprotonation, and activation at the metal-support interface of two supported Au catalysts. Adapting the classic M-M analysis to heterogeneous catalysts provides a useful overall measure of the rate constant for the rate determining step, along with additional insight into potential changes to substrate-support affinity. At the level of analysis performed in this work for a single substrate, the M-M and L-H analyses provided identical results. The multi-sites models and explicit consideration of the surface coverages of different species associated with a L-H analysis offers advantages for heterogeneous catalysts, but the simplicity of the M-M approach and its wide acceptance in many different catalysis communities makes it powerful. The M-M approach revealed a number of nuances associated with applying this analysis to heterogeneous systems. Competitive adsorption on the support and at the active site must be considered in order to ensure that extracted rate constants are not biased against the more weakly adsorbing substrate in multi-substrate experiments. The M-M approach also afforded the opportunity to more carefully consider the assumptions behind Hammett studies of heterogeneous catalysts, most notably that the number of active sites is constant for all substrates. While this is a reasonable assumption from the standpoint of the catalyst, changes to any pre-equilibria before the rate determining step must also be considered. In the particular case of benzyl alcohol oxidation, where alcohol deprotonation is required prior to rate determining hydride transfer, electronic changes to the substrate impact the surface coverage of the active intermediate. Since the measured rate depends both on the coverage of that intermediate and the rate constant for the slow step, changes to the surface coverage of the key intermediate should be considered in order to make more accurate measurements of the key rate constant.

Supporting Information

Complete experimental section, TEM and STEM characterization data, reaction optimization, uncertainty estimation, yield versus time graphs for the rates presented in the saturation plots, mass transfer test, Lineweaver-Burk plots, and numerical analysis of the effects of substrate acidity on alkoxide concentration are presented in the supporting information.

Acknowledgements

The authors gratefully acknowledge the National Science Foundation (Grant CHE-1566301 to BDC and CHE-1565843 to RNA) and the Research Corporation for Science Advancement for supporting this work. We thank Profs. Brian Frederick, Thomas Schwartz, Christina Vizcarra, and Dina Merrer for fruitful conversations as well as the anonymous reviewers. We thank Dr. Amir Zangiabadi for assistance with TEM. BDC thanks Profs. Jeff Bode and Christophe Copéret as well as the Laboratorium für Organische Chemie and the Laboratorium für Anorganische Chemie at ETH Zürich for support during his academic leave.

References

1. Nelson, R. C.; Baek, B.; Ruiz, P.; Goundie, B.; Brooks, A.; Wheeler, M. C.; Frederick, B. G.; Grabow, L. C.; Austin, R. N., *ACS Catal.* Experimental and Theoretical Insights into the Hydrogen-Efficient Direct Hydrodeoxygenation Mechanism of Phenol over Ru/TiO_2 **2015,** 5, 6509-6523.
2. Larmier, K.; Liao, W.-C.; Tada, S.; Lam, E.; Verel, R.; Bansode, A.; Urakawa, A.; Comas-Vives, A.; Copéret, C., *Angew Chem Int Ed Engl* CO_2-to-Methanol Hydrogenation on Zirconia-Supported Copper Nanoparticles: Reaction Intermediates and the Role of the Metal–Support Interface **2017,** 56, 2318-2323.
3. Green, I. X.; Tang, W.; Neurock, M.; Yates Jr, J. T., *Angew Chem Int Ed Engl* Low-Temperature Catalytic H_2 Oxidation over Au Nanoparticle/TiO_2 Dual Perimeter Sites **2011,** 50, 10186-10189.
4. Green, I. X.; Tang, W.; McEntee, M.; Neurock, M.; Yates, J. T., *J. Am. Chem. Soc.* Inhibition at Perimeter Sites of Au/TiO_2 Oxidation Catalyst by Reactant Oxygen **2012,** 134, 12717-12723.
5. Hirunsit, P.; Shimizu, K.-i.; Fukuda, R.; Namuangruk, S.; Morikawa, Y.; Ehara, M., *J. Phys. Chem C.* Cooperative H_2 Activation at Ag Cluster/θ-Al_2O_3(110) Dual Perimeter Sites: A Density Functional Theory Study **2014,** 118, 7996-8006.
6. Briggs, N. M.; Barrett, L.; Wegener, E. C.; Herrera, L. V.; Gomez, L. A.; Miller, J. T.; Crossley, S. P., *Nat. Commun.* Identification of active sites on supported metal catalysts with carbon nanotube hydrogen highways **2018,** 9, 3827-3834.

7. Ro, I.; Resasco, J.; Christopher, P., *ACS Catal.* Approaches for Understanding and Controlling Interfacial Effects in Oxide-Supported Metal Catalysts **2018,** 8, 7368-7387.
8. Tew, M. W.; Emerich, H.; van Bokhoven, J. A., *J. Phys. Chem C.* Formation and Characterization of PdZn Alloy: A Very Selective Catalyst for Alkyne Semihydrogenation **2011,** 115, 8457–8465
9. Green, I. X.; Tang, W.; Neurock, M.; Yates, J. T., Jr., *Science* Spectroscopic observation of dual catalytic sites during oxidation of CO on a Au/TiO_2 catalyst **2011,** 333, 736-9.
10. Green, I. X.; Tang, W.; Neurock, M.; Yates, J. T., *Acc. Chem. Res.* Insights into Catalytic Oxidation at the Au/TiO_2 Dual Perimeter Sites **2014,** 47, 805-815.
11. Saavedra, J.; Doan, H. A.; Pursell, C. J.; Grabow, L. C.; Chandler, B. D., *Science* The critical role of water at the gold-titania interface in catalytic CO oxidation **2014,** 345, 1599-1602.
12. Fujitani, T.; Nakamura, I.; Akita, T.; Okumura, M.; Haruta, M., *Angew Chem Int Ed Engl* Hydrogen Dissociation by Gold Clusters **2009,** 48, 9515-9518.
13. Bruno, J. E.; Dwarica, N. S.; Whittaker, T. N.; Hand, E. R.; Guzman, C. S.; Dasgupta, A.; Chen, Z.; Rioux, R. M.; Chandler, B. D., *ACS Catal.* Supported Ni–Au Colloid Precursors for Active, Selective, and Stable Alkyne Partial Hydrogenation Catalysts **2020,** 10, 2565-2580.
14. Corma, A.; Concepción, P.; Serna, P., *Angew Chem Int Ed Engl* A different reaction pathway for the reduction of aromatic nitro compounds on gold catalysts **2007,** 46, 7266-9.
15. Boronat, M.; Concepción, P.; Corma, A., *J. Phys. Chem C.* Unravelling the Nature of Gold Surface Sites by Combining IR Spectroscopy and DFT Calculations. Implications in Catalysis **2009,** 113, 16772-16784.
16. Widmann, D.; Behm, R. J., *Acc. Chem. Res.* Activation of Molecular Oxygen and the Nature of the Active Oxygen Species for CO Oxidation on Oxide Supported Au Catalysts **2014,** 47, 740-749.
17. Yan, T.; Gong, J.; Flaherty, D. W.; Mullins, C. B., *J. Phys. Chem C.* The Effect of Adsorbed Water in CO Oxidation on $Au/TiO_2(110)$ **2011,** 115, 2057-2065.
18. Masoud, N.; Delannoy, L.; Schaink, H.; van der Eerden, A.; de Rijk, J. W.; Silva, T. A. G.; Banerjee, D.; Meeldijk, J. D.; de Jong, K. P.; Louis, C.; de Jongh, P. E., *ACS Catal.* Superior Stability of Au/SiO_2 Compared to Au/TiO_2 Catalysts for the Selective Hydrogenation of Butadiene **2017,** 7, 5594-5603.
19. Montemore, M. M.; van Spronsen, M. A.; Madix, R. J.; Friend, C. M., *Chemical Reviews* O_2 Activation by Metal Surfaces: Implications for Bonding and Reactivity on Heterogeneous Catalysts **2018,** 118, 2816-2862.
20. Ye, R.; Mao, X.; Sun, X.; Chen, P., *ACS Catal.* Analogy between Enzyme and Nanoparticle Catalysis: A Single-Molecule Perspective **2019,** 9, 1985-1992.
21. Saavedra, J.; Pursell, C. J.; Chandler, B. D., *J. Am. Chem. Soc.* CO Oxidation Kinetics over Au/TiO_2 and Au/Al_2O_3 Catalysts: Evidence for a Common Water-Assisted Mechanism **2018,** 140, 3712-3723.
22. Mao, X.; Liu, C.; Hesari, M.; Zou, N.; Chen, P., *Nature Chemistry* Super-resolution imaging of non-fluorescent reactions via competition **2019,** 11, 687-694.
23. Naidja, A.; Huang, P. M., *Surface Science* Significance of the Henri–Michaelis–Menten theory in abiotic catalysis: catechol oxidation by δ-MnO_2 **2002,** 506, L243-L249.
24. Augustine, R. L.; Doyle, L. K., *J. Catal.* The Platinum-Catalyzed Oxidation of 2-Propanol **1993,** 141, 58-70.

25. Long, C. G.; Gilbertson, J. D.; Vijayaraghavan, G.; Stevenson, K. J.; Pursell, C. J.; Chandler, B. D., *J. Am. Chem. Soc.* Kinetic Evaluation of Highly Active Supported Gold Catalysts Prepared from Monolayer-Protected Clusters: An Experimental Michaelis−Menten Approach for Determining the Oxygen Binding Constant during CO Oxidation Catalysis **2008,** 130, 10103-10115.
26. Fristrup, P.; Tursky, M.; Madsen, R., *Org. Biomol. Chem.* Mechanistic investigation of the iridium-catalysed alkylation of amines with alcohols **2012,** 10, 2569-2577.
27. Mueller, J. A.; Goller, C. P.; Sigman, M. S., *J. Am. Chem. Soc.* Elucidating the Significance of β-Hydride Elimination and the Dynamic Role of Acid/Base Chemistry in a Palladium-Catalyzed Aerobic Oxidation of Alcohols **2004,** 126, 9724-9734.
28. Dijksman, A.; Marino-González, A.; Mairata i Payeras, A.; Arends, I. W. C. E.; Sheldon, R. A., *J. Am. Chem. Soc.* Efficient and Selective Aerobic Oxidation of Alcohols into Aldehydes and Ketones Using Ruthenium/TEMPO as the Catalytic System **2001,** 123, 6826-6833.
29. Thorson, M. K.; Klinkel, K. L.; Wang, J.; Williams, T. J., *Eur. J. Inorg. Chem.* Mechanism of Hydride Abstraction by Cyclopentadienone-Ligated Carbonylmetal Complexes (M = Ru, Fe) **2009,** 2009, 295-302.
30. Samuelsen, Simone V.; Santilli, C.; Ahlquist, M. S. G.; Madsen, R., *Chem Sci* Development and mechanistic investigation of the manganese(iii) salen-catalyzed dehydrogenation of alcohols **2019,** 10, 1150-1157.
31. Mueller, J. A.; Jensen, D. R.; Sigman, M. S., *J. Am. Chem. Soc.* Dual Role of (−)-Sparteine in the Palladium-Catalyzed Aerobic Oxidative Kinetic Resolution of Secondary Alcohols **2002,** 124, 8202-8203.
32. Pirrung, M. C.; Morehead, A. T., *J. Am. Chem. Soc.* Saturation Kinetics in Dirhodium(II) Carboxylate-Catalyzed Decompositions of Diazo Compounds **1996,** 118, 8162-8163.
33. Collier, V. E.; Ellebracht, N. C.; Lindy, G. I.; Moschetta, E. G.; Jones, C. W., *ACS Catal* Kinetic and Mechanistic Examination of Acid–Base Bifunctional Aminosilica Catalysts in Aldol and Nitroaldol Condensations **2016,** 6, 460-468.
34. Wisser, F. M.; Berruyer, P.; Cardenas, L.; Mohr, Y.; Quadrelli, E. A.; Lesage, A.; Farrusseng, D.; Canivet, J., *ACS Catal.* Hammett Parameter in Microporous Solids as Macroligands for Heterogenized Photocatalysts **2018,** 8, 1653-1661.
35. Finiels, A.; Geneste, P.; Moreau, C., *J. Mol. Catal. A: Chem.* Transfer of concepts from homogeneous to heterogeneous catalysis: use of Hammett relationships to assess reaction mechanisms and nature of active sites in reactions catalyzed by sulfides, metals, clays and zeolites **1996,** 107, 385-391.
36. Fristrup, P.; Johansen, L. B.; Christensen, C. H., *Catal Lett* Mechanistic Investigation of the Gold-catalyzed Aerobic Oxidation of Alcohols **2008,** 120, 184-190.
37. Kumar, G.; Tibbitts, L.; Newell, J.; Panthi, B.; Mukhopadhyay, A.; Rioux, R. M.; Pursell, C. J.; Janik, M.; Chandler, B. D., *Nature Chemistry* Evaluating differences in the active-site electronics of supported Au nanoparticle catalysts using Hammett and DFT studies **2018,** 10, 268-274.
38. Johnson, J. B.; Bäckvall, J.-E., *J. Org. Chem* Mechanism of Ruthenium-Catalyzed Hydrogen Transfer Reactions. Concerted Transfer of OH and CH Hydrogens from an Alcohol to a (Cyclopentadienone)ruthenium Complex **2003,** 68, 7681-7684.

39. Steinhoff, B. A.; Guzei, I. A.; Stahl, S. S., *J. Am. Chem. Soc.* Mechanistic Characterization of Aerobic Alcohol Oxidation Catalyzed by $Pd(OAc)_2$/Pyridine Including Identification of the Catalyst Resting State and the Origin of Nonlinear [Catalyst] Dependence **2004,** 126, 11268-11278.
40. Mueller, J. A.; Sigman, M. S., *J. Am. Chem. Soc.* Mechanistic Investigations of the Palladium-Catalyzed Aerobic Oxidative Kinetic Resolution of Secondary Alcohols Using (−)-Sparteine **2003,** 125, 7005-7013.
41. Abad, A.; Corma, A.; García, H., *Chem. – Eur. J.* Catalyst Parameters Determining Activity and Selectivity of Supported Gold Nanoparticles for the Aerobic Oxidation of Alcohols: The Molecular Reaction Mechanism **2008,** 14, 212-222.
42. Conte, M.; Miyamura, H.; Kobayashi, S.; Chechik, V., *J. Am. Chem. Soc.* Spin Trapping of Au−H Intermediate in the Alcohol Oxidation by Supported and Unsupported Gold Catalysts **2009,** 131, 7189-7196.
43. Zope, B. N.; Hibbitts, D. D.; Neurock, M.; Davis, R. J., *Science* Reactivity of the Gold/Water Interface During Selective Oxidation Catalysis **2010,** 330, 74-78.
44. Muñoz-Santiburcio, D.; Farnesi Camellone, M.; Marx, D., *Angew Chem Int Ed Engl* Solvation-Induced Changes in the Mechanism of Alcohol Oxidation at Gold/Titania Nanocatalysts in the Aqueous Phase versus Gas Phase **2018,** 57, 3266-3266.
45. Ide, M. S.; Davis, R. J., *Acc. Chem. Res.* The Important Role of Hydroxyl on Oxidation Catalysis by Gold Nanoparticles **2014,** 47, 825-833.
46. Savara, A.; Chan-Thaw, C. E.; Sutton, J. E.; Wang, D.; Prati, L.; Villa, A., *ChemCatChem* Molecular Origin of the Selectivity Differences between Palladium and Gold–Palladium in Benzyl Alcohol Oxidation: Different Oxygen Adsorption Properties **2017,** 9, 253-257.
47. Campbell, C. T., *Nature Chemistry* Electronic perturbations **2012,** 4, 597-598.
48. Pacchioni, G.; Freund, H.-J., *Chem Soc. Rev.* Controlling the charge state of supported nanoparticles in catalysis: lessons from model systems **2018,** 47, 8474-8502.
49. Desai, L. V.; Stowers, K. J.; Sanford, M. S., *J. Am. Chem. Soc.* Insights into Directing Group Ability in Palladium-Catalyzed C−H Bond Functionalization **2008,** 130, 13285-13293.
50. Campestrini, S.; Cagnina, A., *J. Mol. Catal. A: Chem.* A mechanistic study on oxidation of benzylic alcohols with PPh4HSO5 catalysed by manganese(III) porphyrins in homogeneous solution **1999,** 150, 77-86.
51. Zanella, R.; Giorgio, S.; Henry, C. R.; Louis, C., *J. Phys. Chem B* Alternative Methods for the Preparation of Gold Nanoparticles Supported on TiO_2 **2002,** 106, 7634-7642.
52. Ivanova, S.; Pitchon, V.; Petit, C., *J. Mol. Catal. A: Chem.* Application of the direct exchange method in the preparation of gold catalysts supported on different oxide materials **2006,** 256, 278-283.
53. Panthi, B.; Mukhopadhyay, A.; Tibbitts, L.; Saavedra, J.; Pursell, C. J.; Rioux, R. M.; Chandler, B. D., *ACS Catal.* Using Thiol Adsorption on Supported Au Nanoparticle Catalysts to Evaluate Au Dispersion and the Number of Actives Sites for Benzyl Alcohol Oxidation **2015,** 5, 2232-2241.
54. Kwon, Y.; Lai, S. C. S.; Rodriguez, P.; Koper, M. T. M., *J. Am. Chem. Soc.* Electrocatalytic Oxidation of Alcohols on Gold in Alkaline Media: Base or Gold Catalysis? **2011,** 133, 6914-6917.
55. Carrasco, J.; Liu, W.; Michaelides, A.; Tkatchenko, A., *J. Chem. Phys.* Insight into the description of van der Waals forces for benzene adsorption on transition metal (111) surfaces **2014,** 140, 084704/1.

56. Yildirim, H.; Greber, T.; Kara, A., *J. Phys. Chem. C* Trends in Adsorption Characteristics of Benzene on Transition Metal Surfaces: Role of Surface Chemistry and van der Waals Interactions **2013,** 117, 20572-20583.
57. Molina, L. M.; Lopez, M. J.; Alonso, J. A., *Chem. Phys. Lett.* Interaction of aromatic molecules with small gold clusters. **2017,** 684, 91-96.
58. Reckien, W.; Eggers, M.; Bredow, T., *Beilstein J. Org. Chem* Theoretical study of the adsorption of benzene on coinage metals **2014**, 1775-1784.
59. Xu, B.; Madix, R. J.; Friend, C. M., *J. Am. Chem. Soc.* Achieving Optimum Selectivity in Oxygen Assisted Alcohol Cross-Coupling on Gold **2010,** 132, 16571-16580.
60. Rodriguez-Reyes, J. C. F.; Siler, C. G. F.; Liu, W.; Tkatchenko, A.; Friend, C. M.; Madix, R. J., *J. Am. Chem. Soc.* van der Waals Interactions Determine Selectivity in Catalysis by Metallic Gold **2014,** 136, 13333-13340.
61. Karakalos, S.; Xu, Y.; Cheenicode Kabeer, F.; Chen, W.; Rodríguez-Reyes, J. C. F.; Tkatchenko, A.; Kaxiras, E.; Madix, R. J.; Friend, C. M., *J. Am. Chem. Soc.* Noncovalent Bonding Controls Selectivity in Heterogeneous Catalysis: Coupling Reactions on Gold **2016,** 138, 15243-15250.
62. Personick, M. L.; Madix, R. J.; Friend, C. M., *ACS Catal.* Selective Oxygen-Assisted Reactions of Alcohols and Amines Catalyzed by Metallic Gold: Paradigms for the Design of Catalytic Processes **2017,** 7, 965-985.
63. Takahashi, S.; Cohen, L. A.; Miller, H. K.; Peake, E. G., *J. Org. Chem* Calculation of the pKa Values of Alcohols from sigma* Constants and from the Carbonyl Frequencies of Their Esters **1971,** 36, 1205-1209.
64. Hammond, G. S., *J. Am. Chem. Soc.* A Correlation of Reaction Rates **1955,** 77, 334-338.